J. Coat. Technol. Res.
https://doi.org/10.1007/s11998-021-00518-5

Assessment of sparkle and graininess in effect coatings using a high-resolution gonioreflectometer and psychophysical studies

Jiří Filip, Radomír Vávra, Martina Kolafová, Frank J. Maile

Received: 7 December 2020 / Revised: 17 May 2021 / Accepted: 30 May 2021

Abstract The aim of this article is to propose a model to automatically predict visual judgement of sparkle and graininess of special effect pigments used in industrial coatings. Many applications in the paint and coatings, printing and plastics industry rely on multi-angle color measurements with the aim of properly characterizing the appearance, i.e., the color and texture of the manufactured surfaces. However, when it comes to surfaces containing effect pigments, these methods are in many cases insufficient and it is particularly texture characterization methods that are needed. There are two attributes related to texture that are commonly used: (1) diffuse coarseness or graininess and (2) sparkle or glint impression. In this paper, we analyzed visual perception of both texture attributes using two different psychophysical studies of 38 samples painted with effect coatings including different effect pigments and 31 test persons. Our previous work has shown a good agreement between a study using physical samples with one that uses high-resolution photographs of these sample surfaces. We have also compared the perceived (1) graininess and (2) sparkle with the performance of two commercial instruments that are capable of capturing both attributes. Results have shown a good correlation between the instruments' readings and the psychophysical studies. Finally, we implemented computational models predicting these texture attributes that have a high correlation with the instrument readings as well as the psychophysical data. By linear scaling of the predicted data using instruments readings, one can use the proposed model for the prediction of graininess and both static and dynamic sparkle values.

Keywords Sparkle, Graniness, Psychophysics, Gonioreflectometer

J. Filip (✉), R. Vávra, M. Kolafová
The Czech Academy of Sciences, Institute of Information Theory and Automation, Prague, Czech Republic
e-mail: filipj@utia.cas.cz

F. J. Maile
Schlenk Metallic Pigments GmbH, Roth-Barnsdorf, Germany

Introduction

The texture of visible effect pigment particles is one of the important features for effect coatings characterization. Although a standard for measuring and analyzing coating texture is still missing, the paint and coatings, printing and plastics industries have rountinely been using texture features for quality control purposes for almost a decade. These two features describing coating texture are *graininess* and *sparkle*. While *graininess* (often denoted as diffuse coarseness) characterizes visibility of particles for diffuse illumination, the *sparkle* is related to the number of sparkling particles per unit of paint surface area and their intensity (for a fixed directional illumination often denoted as glint impression, see Fig. 1). Although there is no standard for capturing and evaluating graininess and sparkle, one of the suggested definitions of graininess is: *The sensation of non-uniformity in a surface produced in the consciousness of the observer only when such a surface is viewed under diffuse or partially diffuse illumination.* Similarly, one of the sparkle definitions is: *The sensation of randomly distributed, unstable and highly-luminous objects on a more extended and darker surface with uncorrelated lightness.*

Despite wide usage of these texture features in industry, their relation to computational visual qualities of effect coatings is unknown. In our recent study,[1] we compared differences in the so-called perceived sparkle effect in physical samples painted with effect

Published online: 10 September 2021

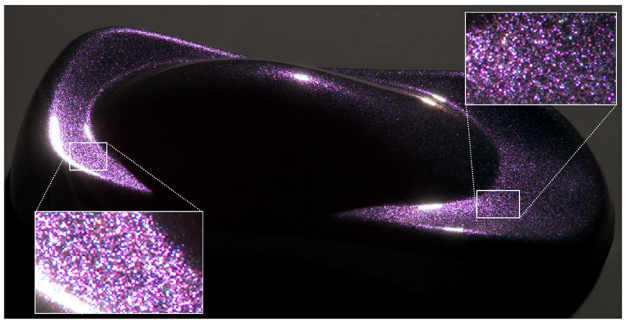

Fig. 1: An example of sparkle in effect coating

coatings using different effect pigment particles, paint systems, colors and pigment particles size. We used a set of 38 samples and performed psychophysical studies on physical samples and their high-resolution photographs, obtained using a goniometric setup. Our comparison has shown a positive agreement between results obtained from both studies and demonstrates that the captured data can serve as an accurate representation of the physical samples.

The purpose of this paper was to use psychophysical studies to assess to what extent goniometric image data can be used to substitute real samples of effect coatings without losing visual information on sparkle and graininess, and how such data relate to readings of commercial devices capable of analyzing these qualities.

In this paper, we build on these results and, through a set of psychophysical studies, we analyzed the perceived graininess and sparkle and

- Compared results of the psychophysical assessment with readings of two commercially available instruments,
- Tested computational models of graininess and static sparkle providing a reliable fit with the psychophysical data,
- Analyzed dynamic sparkle effect and proposed an approach to its computational characterization.

This paper is organized as follows: In ''Related work'' section, we discuss related work. ''Tested coatings'' section introduces our test sample set. ''Methodology'' section explains methodology of our psychophysical tests. ''Experiments'' section shows the results of psychophysical studies on real samples and their photographs. ''Comparison to industrial devices'' section compares psychophysical judgments of sparkle and graininess to readings of commercial devices. ''Prediction of sparkle and graininess'' section demonstrates performance of computational models of sparkle and graininess on the test dataset. Finally, in ''Implication to dynamic sparkle model'' section, we compare perceived dynamic sparkle with a suggested computational model. ''Conclusions'' section discusses the achieved results and includes directions for future work.

Related work

One of the first surveys on applications of angle-dependent optical effects deriving from sub-micron structures of films and pigments was presented.[2] Effect pigments can be, based on the principle of chroma and sparkling effect generation, roughly divided into three categories that in practice, are often combined in coating systems:[3,4] (1) *metallic pigments* relying mainly on geometrical properties of pigment flakes and their reflectance, (2) *interference pigments* where color effects are caused by light wave interference with a transparent substrate coated with materials of high refractive indices, and (3) *diffractive pigments* decomposing light at a diffraction grating of a frequency close to the wavelength of the incoming light.

As the main goal of this paper is to analyze the relationship between the real and captured texture of effect coatings, and its assessment of sparkle and graininess in effect coatings using commercial devices, we overview topics on (1) coatings texture analysis, (2) methods of effect coatings modelling, and (3) industrial characterization of coatings textures.

Visual assessment of effect coatings textures

The texture effect of special effect coatings has been studied for several decades. Kitaguchi et al.[5] assessed graininess of metallic coatings on real specimens and their photographs and concluded that there is no difference in accuracy regardless of the photographed area magnification. Kirchner et al.[6] applied psychophysical tests to identify a diffuse coarseness and glint impression under either diffuse or directional lighting as important texture features of effect coatings. They have shown that trained observers can distinguish between 8 and 10 levels of such features with high mutual consistency. Observers' repeatability and reproducibility were around 0.5 on an eight point scale. Huang et al.[7] proposed a method predicting total visual differences of effect coatings based on variations in color, coarseness, and glint impression. The method depends on the type of illumination used. Rentschler[8] has shown a systematic variation of sparkle and graininess for different effect pigment types and particle sizes. Dekker et al.[9] psychophysically analyzed color, sparkle and graininess and used the information to derive a total appearance difference equation. The Kirchner and Ravi[10] overview recommended color and texture tolerances appropriate for use in the automotive industry. For coating texture, they report a sparkle grade parameter introduced by the BYK-Gardner company, defined as a geometrical mean of sparkle intensity and sparkle area. Kirchner et al.[11] borrowed a

motivation from astronomy and used it for predicting the number of visually distinguishable flake intensities. Wang and Luo[12] ran several psychophysical studies to validate sparkle and graininess readings of the BYK-mac commercial device by BYK-Gardner company. Seubert et al.[13] analyzed the relationship between flake orientation and coating appearance and created a model of scattering behavior for metallic paint systems.[14]

Gómez et al.[15] compared human observations of sparkle to the sparkle readings of BYK-mac device. They found a good correlation to the sparkle grade for geometry 45°/aspecular 45° intensity, but much worse correlation for sparkle intensity and area.

Wang and Luo[12] carried out visual studies for diffuse coarseness and glint impression and compared the psychophysical data to readings of the BYK-mac instrument. By data dimensionality analysis of the sparkle space by means of multi-dimensionl scaling, they identified two main dimensions related to the sparkle intensity and sparkle area. They concluded that the glint impression is highly related to the particle size of the effect pigment used, which is the main factor controlling the sparkle intensity, alongside full width at half-maximum (FWHM) obtained from dense multi-angle BRDF measurements.

Iacomussi et al.[16] psychophysically analyzed the sparkle effect of mica-based effect pigments of different particle size distributions under different illumination conditions and compared the results with readings of the BYK-mac instrument.

Visual effects of dynamic behavior of sparkle pattern have not been studied in depth so far. Kirchner et al.[6] pointed out the importance of the dynamic character of glints and suggested the analysis of the visibility of a particular glint spot depending on the angle of illumination. Filip et al.[1] have shown an experiment with 38 samples where there are significant differences between perceived static sparkle obtained as and image and dynamic sparkle obtained as a collection of images for different illumination polar angles.

New approaches to measurement and visual assessment of texture features of effect coatings have emerged in recent years. Amookht et al.[17] used a scanner to characterize visual coarseness of silver and blue metallic coatings. Authors tested several analytical methods such as the auto-correlation function and the wavelet transformation and have shown their agreement with data obtained from visual studies. Watanabe[18] constructed a device that evaluates the multi-angle sparkle impression in one shot, based on a line spectral camera, light source, and motorized rotation stage. He developed a method for quantifying the sparkle impression based on spatial frequency characteristics and confirmed a good correlation to visual studies and the MA-T12 instrument by X-Rite. Perales et al.[19] evaluated graininess captured by the BYK-mac instrument using visual scaling constructed by the rank-order and paired-comparison psychophysical methods. After visual scaling, authors achieved good correlation between both magnitudes. Ferrero et al.[20] presented the current progress in the definition of traceable sparkle measurands and their measurement by several national metrology institutes. This work introduces a complete guidance for sparkle definition and measurement, experimentally supported by a good match between measurement and visual data.

Modeling and visualization of texture effects of effect coatings

One of the first attempts at the modeling of these materials by means of the BRDF model was done by Günther et al.[21], where the spatial sparkle effect was introduced using either a physical[22] or statistical[23,24] model of sparkling flake sizes and orientations. Later, Ďurikovič and Mihálik[25] introduced a method of separately capturing and fitting BRDF data and spatially varying sparkle effects. More advanced techniques extend to spatially varying appearance representations using the bidirectional texture function (BTF). Rump et al.[26] collected dense BRDF measurements from a large measured sample due to the close proximity of camera and light. They fit the Cook–Torrance model to measured BRDF data and the fitted values were subtracted from all BTF images, providing spatially varying sparkle data further compressed by principal component analysis. At the visualization stage, the BRDF value is combined with a randomly sampled BTF patch. In follow up work, Rump et al.[27] proposed the detailed angular analysis of flake properties using video. The obtained information was used for a proper sampling and example-based compression of the measured BTF of paint. The compression is based on histogram clustering and achieves significantly higher compression rates than the previous approach. Golla and Klein[28] further reduced memory footprint and computational costs of this model to allow real-time high-quality renderings in VR applications. Lans et al.[29] presented an empirical approach to the realistic modeling of special effect flakes which fit patch-based model parameters using sparse texture data obtained by a portable multi-angle spectrophotometer. Kirchner and Ravi[30] related statistical parameters of the paint composition to perceived texture parameters of sparkle and graininess. Ferrero et al.[31] proposed a simple analytical model of sparkle and graininess based on basic parameters of optical system and illumination and observation conditions. Authors studied contrast and density of sparkle spots at different illumination/observation geometries to establish the sparkle/graininess characteristic of a specific effect coating. While the contrast between the sparkle spots and background is determined by the specular reflectance of the flakes, their size and diffuse reflectance of the coating, the density of sparkle spots is determined by the orientation distribution of the

flakes and their flatness. Kirchner et al.[32] proposed a model for effect coating visualization based on a multispectral BRDF, which is capable of rendering sparkle as well as gloss, based on objective measurements of both parameters.

Industrial characterization of texture

Early methods applied to effect coatings characterization back in the seventies and eighties considered only two to four geometries to be sufficient for coating characterization of solid colors.[33] With the onset of effect pigments, more geometries turned out to be necessary and development converged to the acceptance of standard ASTM E 2539-08[34] that was later on further extended to ASTM E 2539-12.[35] Several industrial instruments have been introduced in the last three decades. BYK-mac by BYK-Gardner[36] uses five ASTM in-plane scattering geometries plus an additional view of the geometry 45°/light 15° aspecular. This device pioneered the effect coating texture analysis represented by two proprietary texture features: *graininess* obtained for diffuse illumination, and *sparkle* obtained for three illumination directions and a fixed viewing direction 0°. Such a texture analysis has also been included in the recent instrument MA-T12[37] which captures ASTM geometries plus a further four samples for illumination at 15°. MA-T12 used the Helmholtz reciprocity and substitutes incoming and outgoing directions. Therefore, it features two pickup angles: at 15° and 45° and six illumination directions defined by ASTM geometries. Due to this, the sparkle is evaluated for a viewing angle of 15° and six illumination directions.

In this paper, we compare human observers' visual judgments of sparkle and graininess obtained for real samples and their digital photographs with readings of commercial devices, and outputs of tested computational models.

Tested coatings

For the purpose of our analysis, we collected a set of 38 effect coatings featuring different pigment types, coating systems and basecoat colors. They are listed in Table 2. Each sample has a unique identifier consisting of three letters:

The first letter defines pigment type: **A**—an automotive coating including aluminum flakes of silverdollar morphology with a mean particle size of 15 to 30 μm, **M**—mica, **C**—combines aluminum and mica and pigments with a mean particle size of from 15 to 30 μm, **D**—diffractive coating including a diffractive effect pigment with a mean particle size 20 to 150 μm. **U**—a high-sparkle contrast, pearlescent coating including an ultra-thin, colored aluminum pigment (UTP) with a mean particle size of 21 μm, **V**—a mirror-like, highly-reflective coating based on well-aligned and oriented vacuum metallized pigments (VMPs) with a mean particle size of 12 μm.

All but **V** feature high sparkle contrast due to angularly dependent pigment reflectivity and are highly specular due to a clearcoat used on top of the effect pigmented basecoat layer. The diffractive pigment *D* exhibits a unique, gonioapparent chromaticity due to a regular grating of pigment flakes introduced by means of optical lithography.

The second letter defines the coating system used: **S**—solventborne, **P**—powder coating and **W**—waterborne.

The third letter defines the basecoat color (**B**—black, **W**—white).

If the information is not available, the letter is X. Photographs of the coating panels captured for the point-light source are in Fig. 2. A more detailed description of tested samples is given in the "Appendix". For the majority of samples, we know the mean particle sizes for distributions D10, D50, and D90; however, for those where these values are unknown, we performed a basic analysis of the pigment size. We used the digital optical microscope Bresser Biolux Touch. The optical calibration was done using the NIST traceable glass target with a defined size of dots where one pixel corresponded to 0.36 μm. For each coating, we measured the size of five typical flakes selected manually. Figure 3 shows the average flake sizes for individual coatings tested.

Methodology

In two psychophysical studies, we investigated graininess and sparkle for all 38 samples described in "Tested coatings" section. In both studies, a group of observers assessed the samples and evaluated (1) perceived graininess and (2) sparkle on an eleven-point Likert-like rating scale, where 0 corresponds to the lowest and 10 to the highest intensity. This range should represent only the span of materials within the study, and according to the literature,[6] this should sufficiently cover the visual range of sparkle effect. This design we adopted as it is dominant in image and video experiments.[38]

The observers rated both properties separately for each of the samples investigated. In order to make the perceptual scaling task easier, each stimulus contained all evaluated samples. The observers were aged 22 to 54, all having normal or corrected vision and naive with respect to the purpose of the experiment.

Experiment 1—Real samples

In the first experiment, we placed all test samples on the table labeled with corresponding numbers as shown in Fig. 5. The table was placed near a window.

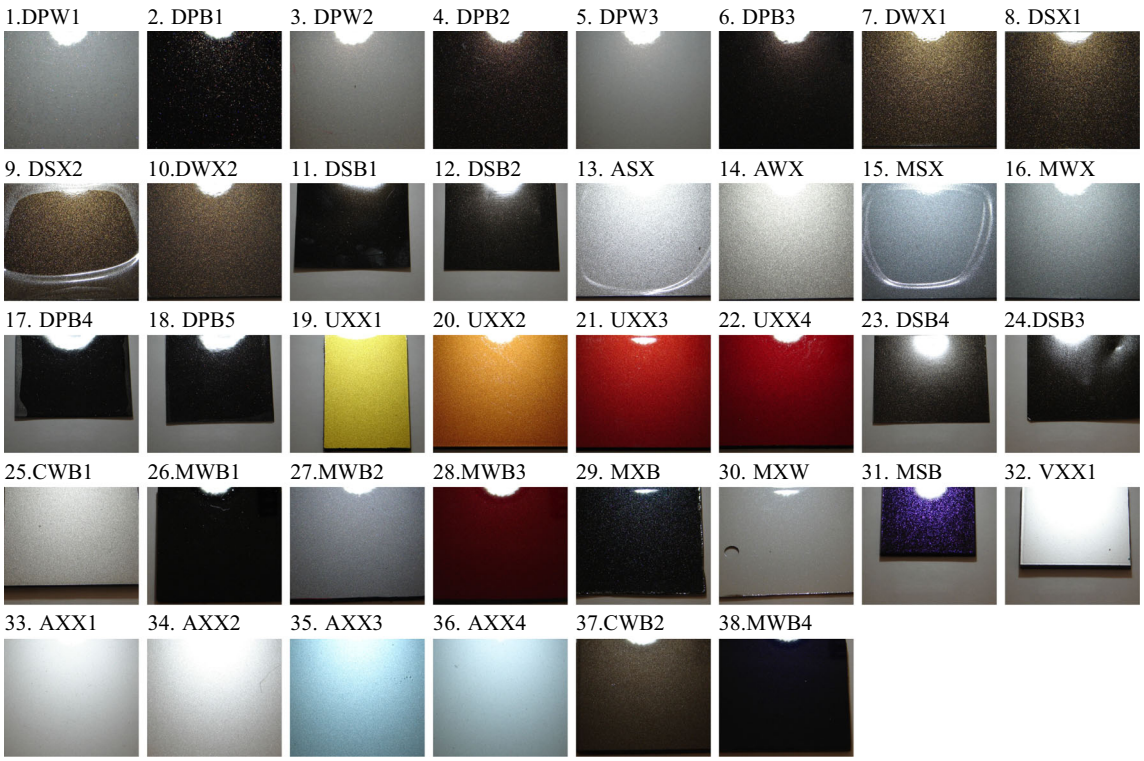

Fig. 2: Photographs of the tested coatings with a point light illumination

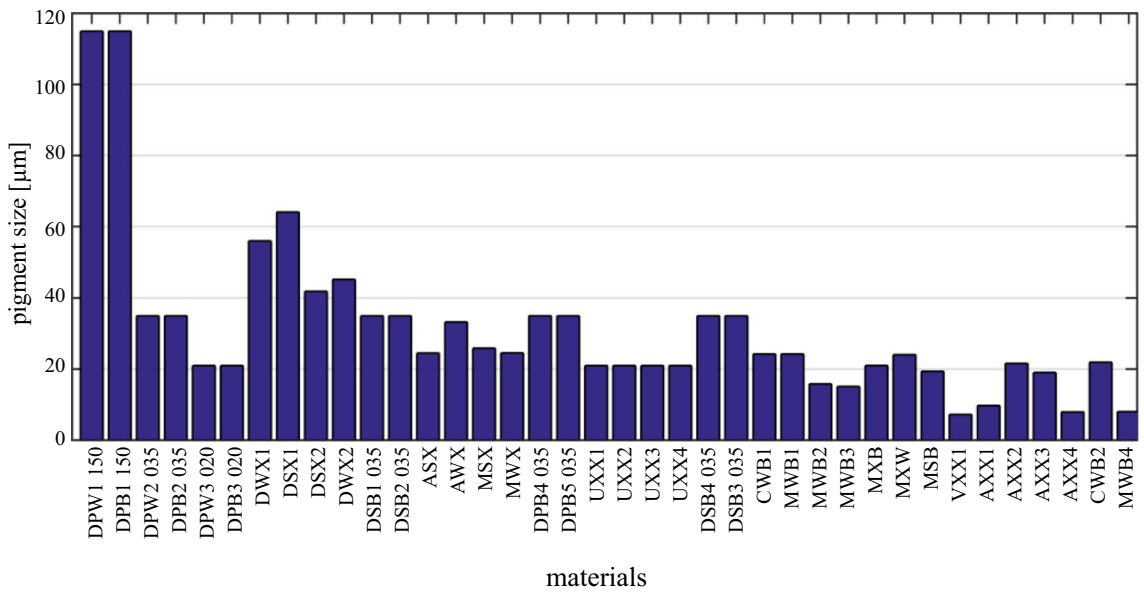

Fig. 3: Measured average effect pigment particle size of the tested coatings using an optical microscope

Graininess was evaluated only under indirect daylight illumination, while sparkle was evaluated under directional illumination using a single warm-white LED lamp (2376 lux, 2700K) in a darkened office environment (see Fig. 4). Observers were allowed to move the samples, but not change the lighting conditions. There was no time restriction on the task. A total of 20 naive observers participated in the experiment. Each session, i.e., the evaluation of graininess and sparkle for each sample, typically took 30 min. The subjects' task for graininess was the following: *Evaluate structure/grain visibility of each sample on a scale from 0–10, where 0 and 10 should correspond to the sample with the lowest and highest visibility*. For sparkle they were asked:

Jointly evaluate the number and intensity of sparkling reflections of each sample on a scale from 0–10, where 0 and 10 should correspond to the sample with the lowest and highest sparkle.

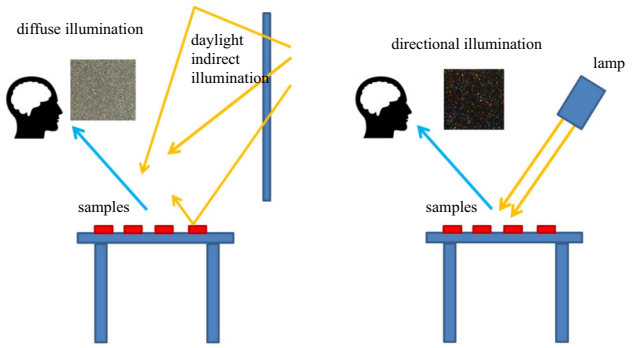

Fig. 4: The design of the experiment set up

Experiment 2—Photographs of samples

In the second experiment, we analyzed perceived sparkle and graininess values to validate if our image-based measurements can directly be used to substitute assessment of real specimens. We used high resolution photographs of the same samples obtained by a

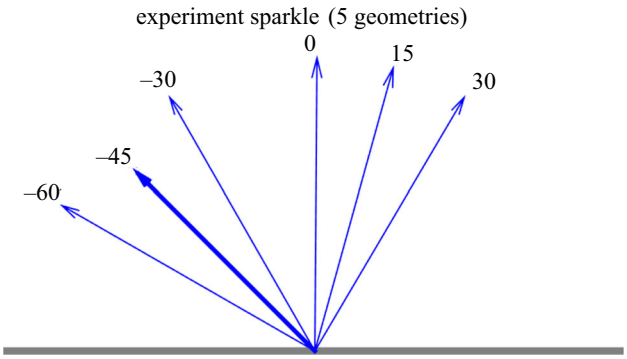

Fig. 6: Geometries used for sparkle analysis in experiment 2

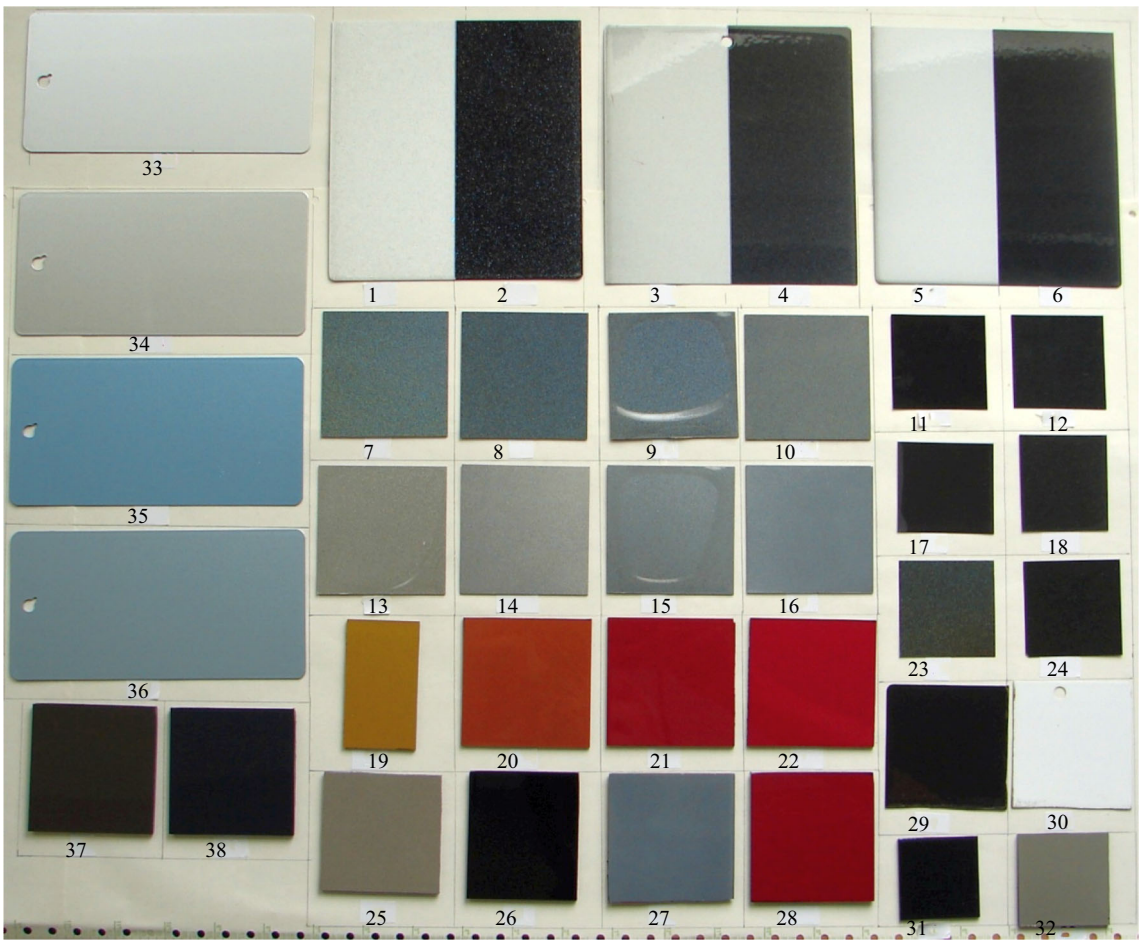

Fig. 5: A table with materials as seen by the observers

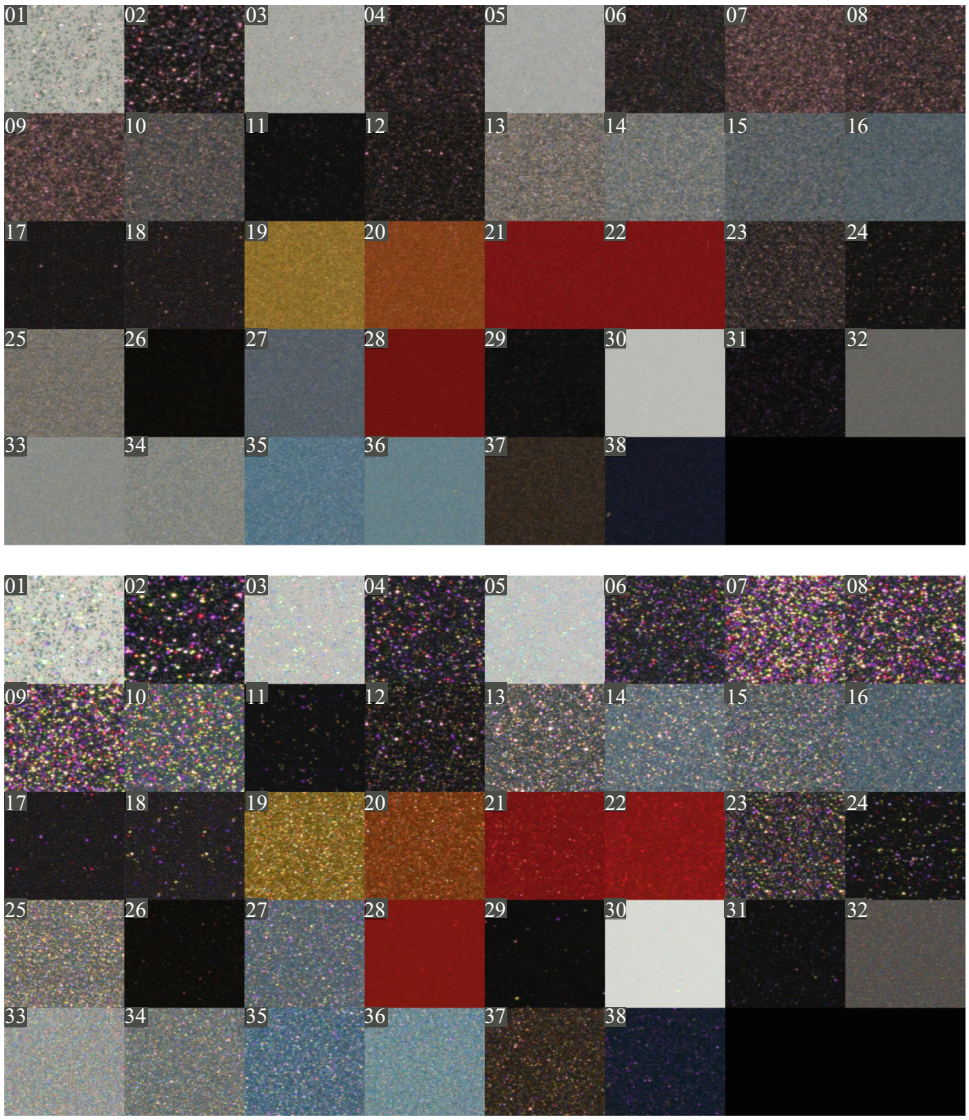

Fig. 7: Examples of stimuli images for graininess (top) and sparkle for $\theta_i = 0^\circ$ (bottom)

goniometer[39] with a 16Mpix RGB camera. The distance of the camera sensor from the sample was 2 m. In our experiments, we used a resolution of 353 dpi (i.e., 67 μm/pixel). We used an in-plane geometry with respect of the viewing polar angle $\theta_v = 45^\circ$ and five illumination polar angles as shown in Fig. 6. We selected the illumination angles in such a way as to obtain the same differences between viewing and illumination directions as those used in commercially available sparkle measuring devices (see Fig. 9). Relative angles to viewing direction were −15°, 15°, 45°, 60°, and 75°. Also, this arrangement is in agreement with the observation[15] that geometry 45°/aspecular 45° has better agreement of user studies to device readings than geometry 15°/aspecular 15°. We captured the images for all 38 materials of our sample set, in five geometries. To obtain an approximation of graininess using our goniometer with a single point light, we captured the images at the in-plane geometries for 151 illumination angles in one degree steps and computed the average value across all 151 images. This approach represents the global illumination using a set of discrete directional lights which is often used for material appearance relighting in computer graphics. Then, photographs of all 38 tested samples were compiled into a single image with a resolution of 1920×1080 pixels, where each subimage 240×240 pixels corresponds to approximately 16 mm^2 of the real specimen. Examples of stimuli images for graininess and sparkle are shown in Fig. 7. Alongside static images, we also prepared dynamic stimuli to assess perceived impression of dynamic sparkle. To this end, we used a video sequence of coatings samples captured from the same viewpoint at elevation 45° with an illumination ranging in-plane between elevations of −75° to 75°, measured at increments of 1°. Subject

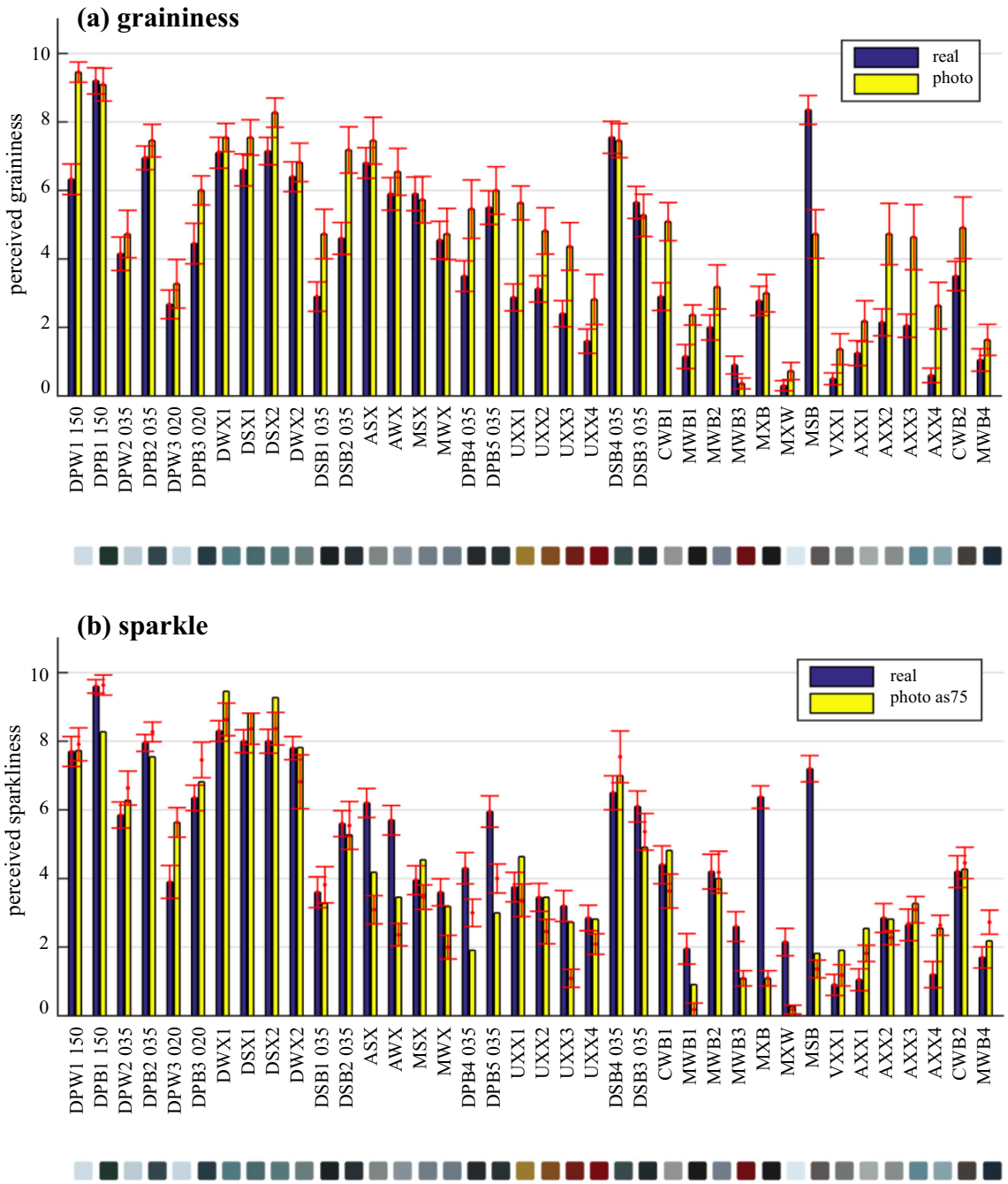

Fig. 8: Values of (a) graininess and (b) sparkle obtained in experiments with real samples and their photographs

again assessed sparkle impression on a scale between 0 and 10.

The stimuli images were shown on a screen of a 24'' color-calibrated studio monitor and the observers assessed (1) graininess and (2) sparkle of individual samples. There was no time restriction on the task. A total of 11 naive observers participated in the experiment. Each session, i.e., evaluation of graininess and five variants of sparkle of each sample, typically took 60 min.

Experiments

This section shows our results for the psychophysical assessment of sparkle and graininess on physical samples as well as their measurements.

Psychophysical evaluation of real samples

Prior to the data analysis, we checked the presence of outliers and assessed agreement across observers. First,

Table 1: Correlations of graininess and sparkle values between experiments using real samples and their photographs for viewing polar angle $\theta_v = 45°$

	Polar	Aspecular	r	p-value
Graininess	–	–	**0.873**	0.0
Sparkle	$\theta_i = -60°$	105°	**0.787**	0.0
Sparkle	$\theta_i = -30°$	75°	**0.774**	0.0
Sparkle	$\theta_i = 0°$	45°	0.684	$2.0e{-6}$
Sparkle	$\theta_i = 15°$	30°	0.331	$4.2e{-2}$
Sparkle	$\theta_i = 30°$	15°	0.616	$3.9e{-5}$

we performed an outliers rejection by removal of values differing from the mean subject response for more than 5 scale points. A total of 39 outliers were found representing 2.4% of the 1520 values recorded in the study.

Next, we checked inter-observers agreement using the Krippensdorff alpha[40]—a statistical measure of the agreement generalizing several known statistics. Output $\alpha_K = 1$ represents an unambiguous indicator of reliability, while 0 does not. The α_K values computed for graininess and sparkle were 0.630 and 0.783, demonstrating good agreement among the observers.

We also analyzed the significance of differences between the mean values for all samples using hypotheses testing of means of individual samples using Kruskal-Wallis repeated measures ANOVA at significance level 0.05. The obtained p-values below 2e–7 for both graininess and sparkle demonstrate high significance.

To get an insight into the typical responses of the observers, we computed the mean opinion score (MOS) obtained as an average rating across all subjects. This is a standard methodology for subjective quality assessment used especially in the audio and video industries, and recommended by international standard organizations such as ITU[41] or ISO.[38] The mean opinion scores in range 0–10 for individual perceptual attributes and tested materials are shown for graininess and sparkle in Fig. 8 in blue. The error bars in the graphs represent the standard error values.

Psychophysical evaluation of photographs

Similarly to the experiment assessing the photographs of samples, we started with outlier detection, identifying 32 outliers representing 1.3% of the 2508 values recorded in the study. The Krippensdorff alpha values computed for graininess were 0.503 and for sparkle 0.790, 0.765, 0.610, 0.599, 0.494, demonstrating a reasonable level agreement among the observers particularly for the first two geometries. We performed hypothesis testing using repeated measures ANOVA at significance level 0.05. We obtained high statistical significance of the results with p-values below 3e–9.

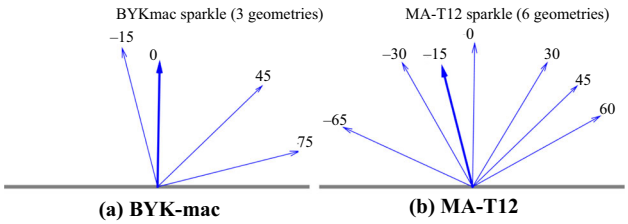

Fig. 9: Geometries used for sparkle evaluation in two commercial devices: (a) BYK-mac, (b) MA-T12

The computed mean opinion score values are shown alongside MOS values from the first experiment in Fig. 8 in blue color.

We also computed correlations between the results for both experiments. Table 1 shows Pearson correlation coefficients computed between results of both experiments (including p-values) (Fig. 8).

The correlation of perceived graininess in real samples and their photographs was relatively high $r = 0.873$; however, we can observe that the UTP pigments (UXX1-4) and some aluminum-based effect pigments (AXX1...AXX4) recorded values that were almost twice as high in the assessment of photographs than of real samples, while for mica-based sample (MSB), we observed the inverse behavior.

We also observed good correlation values for majority of sparkle geometries with the highest values recorded for nearly retro-reflective illumination, i.e., −60° (as 105°), −30° (as 75°). Reasonable correlation was also attained for normal illumination 0° (as 45°). As this illumination geometry is also commonly used in commercial instruments and recommended by other studies,[15] our results for this geometry are shown in Fig. 8 for this geometry. These differences to the assessment of real specimens can be due to two factors. First, the limited camera resolution of our system, that is not able to correctly record behavior of isolated pigments, which are smaller than the covered pixel size. In such a case, high brightness of the pigment particle is projected onto pixel area which is larger than the particle itself. Second, a limited dynamic range of displayed stimuli images can mask faint but sharp glints of lower intensities, that are projected onto a single pixel. This is particularly apparent for samples based on pigments of small particle sizes, e.g., high differences were recorded for mica-based samples (MXB, MXW, MSB) where the sparkle perceived from photographs was much lower than from real samples. We assume that using system with higher DPI would further improve agreement of the responses.

Detailed correlation plots comparing results of both experiments are shown in the first row of Fig. 18.

Discussion of limitations

Although the presented results show that the captured image data reliably preserve sparkle effects, there are

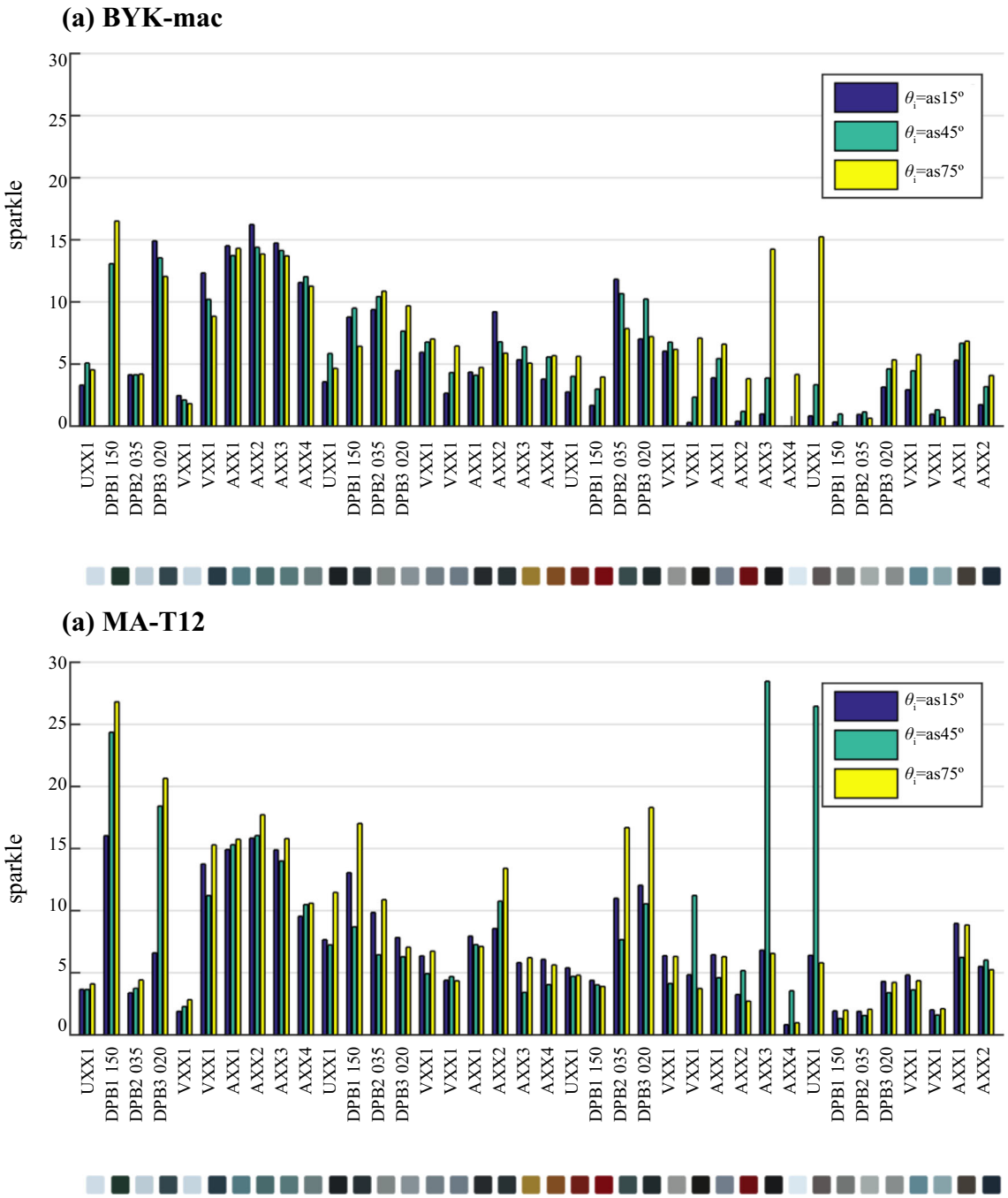

Fig. 10: A comparison of sparkle level values obtained by (a) BYK-mac and (b) MA-T12 for different polar illumination angles

still differences for specific samples. They can be, among others, attributed to the following factors. First, our camera resolution is limited and cannot reliably distinguish between several sparkles of smaller closely located flakes, although this effect is probably not of great importance as our visual system would consider them as one spot.

Second, although our photographs are recorded in high dynamic range (HDR), the color-calibrated studio monitor used in the psychophysical experiments had only limited dynamics that migh have diminished the intensity levels of sparkle spots.

Third, while in the first experiment subjects assessed physical samples of minimal size 5×5 cm^2, in the second experiment, we used only a limited spot of the captured sample corresponding to approximately 0.6×0.6 cm^2. Although Kitaguchi et al.[42] suggested that the size of the sample area presented to the

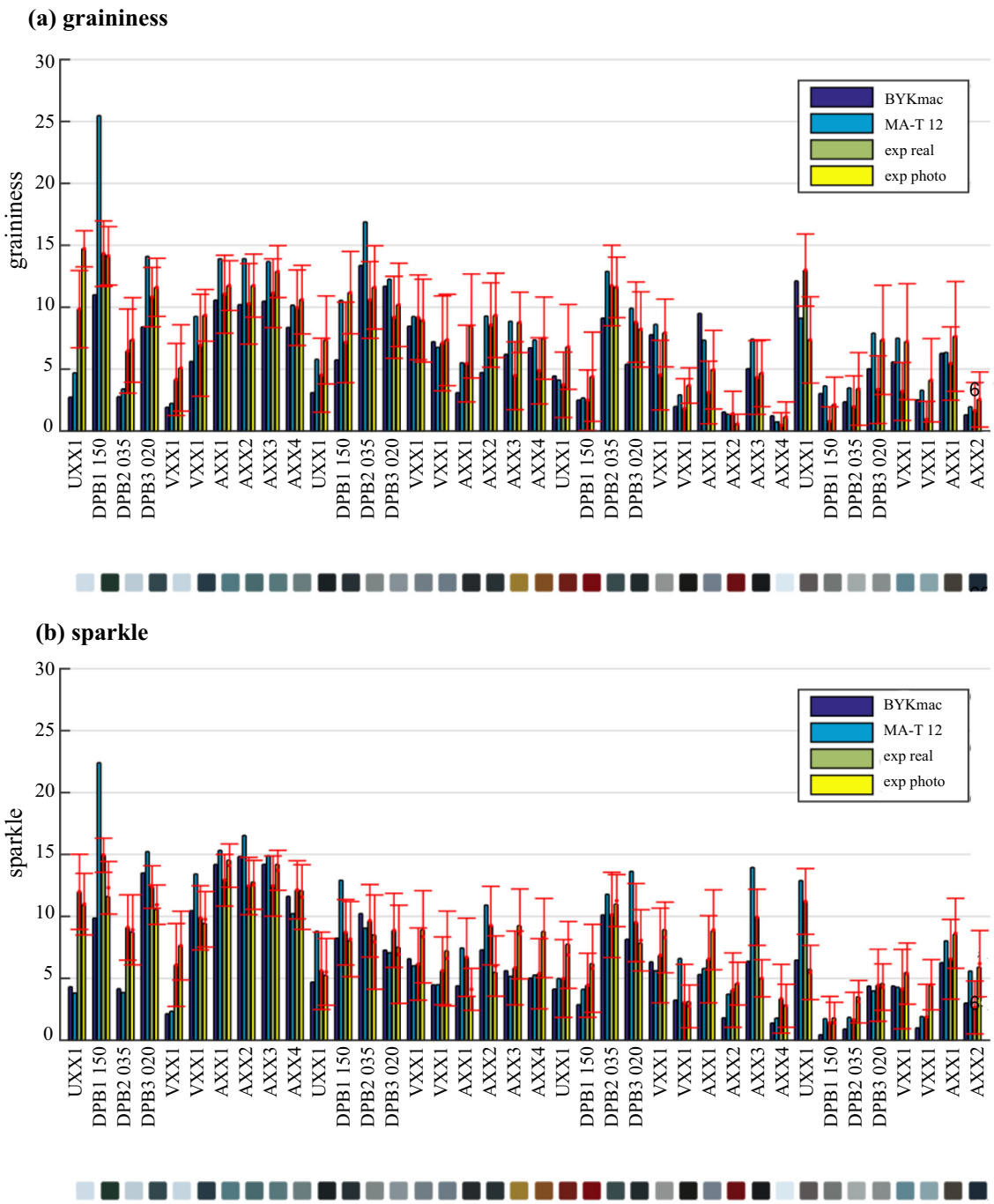

Fig. 11: A comparison of (a) graininess and (b) sparkle values obtained for two tested commercial devices (capturing geometries 0°/45° and 15°/30°) and our psychophysical experiments using real samples and their photographs

observer is not important and observers tend to focus on only a part of the sample, this could make a difference if the selected spot is not representative enough to deliver all modalities which need to be considered under sparkle. As we carefully selected samples which were flawless, and also carefully selected the captured area, and checked the captured image, we assume that we minimized such a risk.

Fourth, the graininess data were obtained by linear combination of contributions of different in-plane lighting directions after an angular step of one degree. This approximate representation of graininess data could also slightly bias our results.

Mean opinion scores of psychophysical data averaged across all subjects are shown in the "Appendix".

Comparison to industrial devices

As mentioned in ''Related work'' section, there are mainly two devices of commercial and technical relevance that are capable of directly measuring graininess and sparkle: the so-called BYK-mac device by BYK-Gardner[36] and MA-T12 by X-Rite.[37] In this section, we compare the performance of these devices with the results from our psychophysical studies.

Sparkle geometries captured by both devices are in the plane of incidence and they are shown in Fig. 9, where the bold arrow stands for the observation direction and the regular arrows for the illumination directions.

As the devices do not capture the same geometries, we assessed sparkle using both devices on the closest geometries. Note that there is a shift of geometries between the devices of 15° as the BYK-mac has a viewing angle of 0°, while MA-T12 has one of −15°. However, the relative angular differences between light and sensor are the same for both devices, while MA-T12 offers recording of two additional illumination angles. Thus, for a direct comparison we used only directions −15°, 45°, and 75° (corresponding to − 30°, 30°, and 60° for MA-T12). Figure 10 shows sparkle values for all three tested geometries. We observed a slightly increasing tendency with an increasing aspecular illumination angle for both devices, and only the BYK-mac readings change this trend for aluminum-based metallic pigment samples AXX2 and AXX3 with 22 μm particle size. When comparing both devices, we observe significantly higher responses from the MA-T12 for the diffractive pigments.

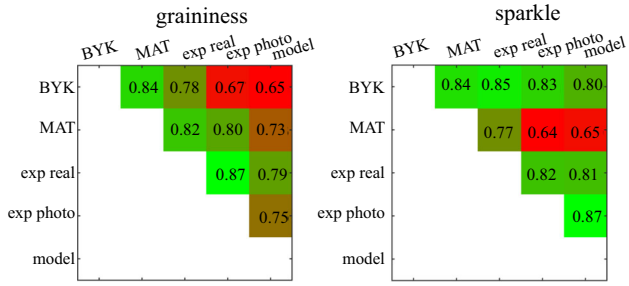

Fig. 12: Correlation of graininess and sparkle values between two commercial devices, results of our psychophysical experiments and the implemented model

To facilitate a comparison of the device performance and the results of our studies, we computed the average sparkle values across all three captured illumination geometries. For our second study, we did the same, i.e., averaged responses for different geometries. Moreover, we had to rescale values from the scale of the psychophysical study, i.e., 0–10 to the absolute scale of the devices. To this end, we performed a linear fit between averaged values from the devices and from the experiments, obtaining scaling constants for both graininess and sparkle. These constants were averaged across all geometries and we obtained similar values $k_s = 2.1$ which we used to rescale the psychophysical values. A side-by-side comparison of graininess and sparkle values between devices and our studies is given in Fig. 11.

Results of our studies perform similarly to readings from the devices. We observed that the scale values obtained from the experiment with captured photographs were generally higher, especially in the case of graininess and aluminum-based effect pigment samples. The agreement of our experiments with the devices' readings was similar for graininess and sparkle, while slightly better for the study using real samples (the Experiment 1).

Finally, we computed the Pearson correlation coefficients between the results for both devices and our two experiments as shown in Fig. 12. Here, we should point out the very good agreement of both devices in both statistics. As said before, the results of the experiment with real specimens were better correlated with the devices than the results of the experiment with photographs, while the MA-T12 achieves better correlation for graininess and BYK-mac for sparkle. Detailed correlation plots comparing results of our

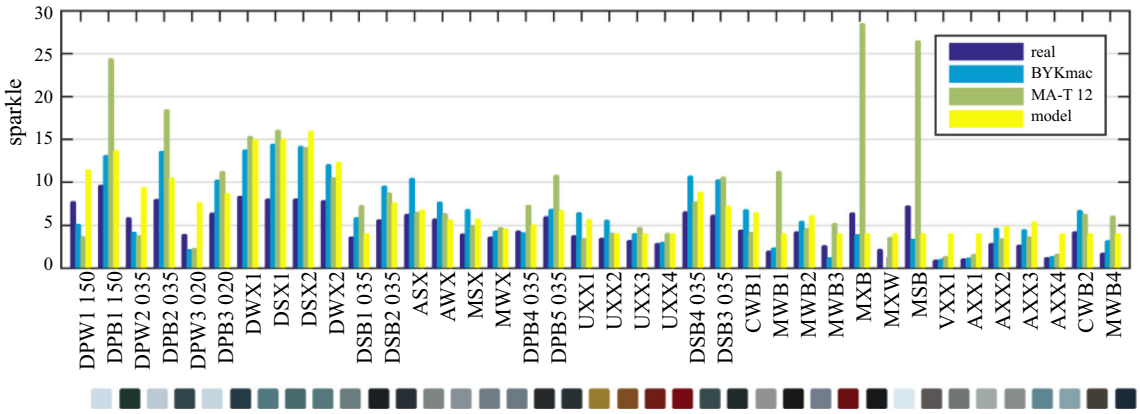

Fig. 13: Sparkle model performance: a comparison of psychophysical data with commercial device readings and with the model's predictions

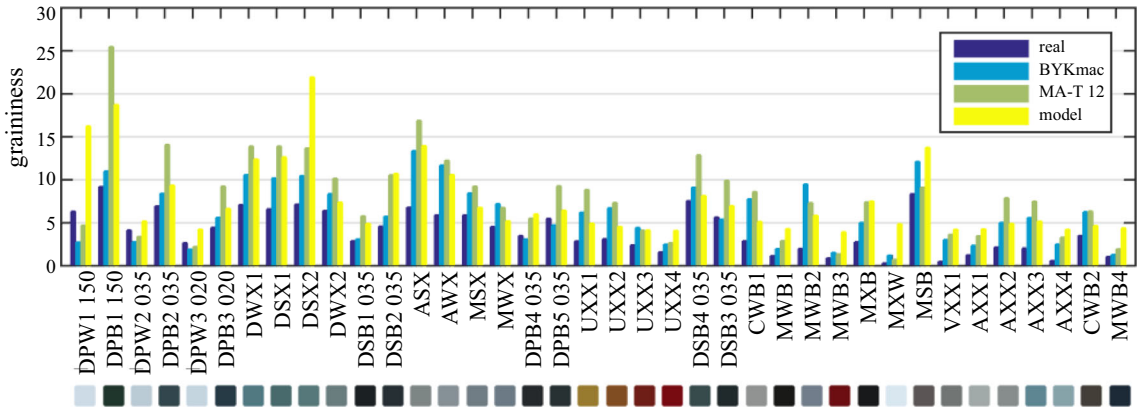

Fig. 14: Graininess model performance: a comparison of psychophysical data with commercial devices readings and with the model's predictions

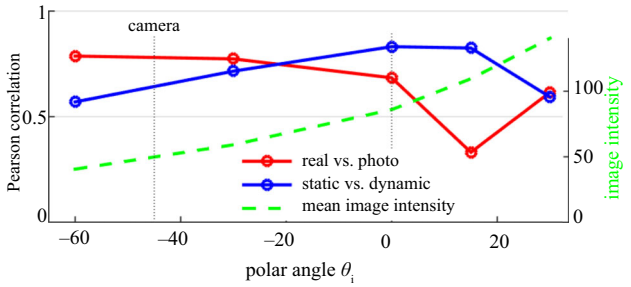

Fig. 15: Pearson correlation between perceived sparkle in: (red) real samples and their photographs taken for different illumination elevations, (blue) static photographs at different elevations versus dynamic sequence. Green outline depicts proportional average luminance of observed materials (Color figure online)

experiments, with readings of both devices are shown in the second, third and fourth row of Fig. 18.

Our studies have show relatively small differences between perception of sparkle and graininess in real samples and their captured photographs. Therefore, we have used only the captured data for testing a computational model of graininess and sparkle suggested in the following section.

Prediction of sparkle and graininess

Sparkle model

As behavior of sparkle in effect coatings has similar properties as the stars in the night sky, we followed the methodology used in astronomy as proposed.[11] In practice, we computed the apparent stellar magnitude[43] of individual image pixels and thresholded it using a fixed threshold m_t

$$2.5\log_{10}\left(\frac{E_0}{E}\right) < m_t, \tag{1}$$

where $E_0 = 2.09e{-}6$ lm/m^2 is the reference illuminance and E is pixel illuminance. The magnitude for the brightest stars has a value $m_A = -4.4$, while for just noticeable stars, it is $m_B = 6$. As we need to detect only the brightest sparkle spots in the coated samples including different effect pigments, we set the magnitude threshold experimentally so it would correspond to 15% of the entire interval, i...., $m_t = 0.15 \cdot (m_A - m_B) = -1.56$. The threshold used may correspond to the difference in contrast between the stars in the sky, and glints in coating that have nonzero ambient background illumination. Further extension of this approach should also take account of the effect of background luminance on the contrast threshold as outlined.[20]

We evaluated three basic quantities of sparkle image pixels selected by thresholding: number of sparkle spots S_c, the typical sparkle intensity S_i, and the pixel area occupied by the sparkle spots S_a. The number of sparkle spots S_c is obtained as a total number of continuous pixel areas in the thresholded image. The sparkle intensity S_i is computed as the apparent stellar magnitude of the median values of sparkle areas. The sparkle area S_a is represented as the percentage of pixels occupied by sparkles related to the entire image area. Finally, a sparkle grade S is defined as a geometric mean of the sparkle area and sparkle intensity, i.e., $S = \sqrt{S_i \cdot S_a}$.[10]

We compared this model performance with the psychophysical data obtained from the assessment of physical samples and their HDR photographs. We used the illumination polar angle 0° (45° aspecular). A Pearson correlation for the estimated sparkle grade to sparkle assessed from real samples was 0.812 and to sparkle assessed from captured images was 0.869.

Although the model provides a promising performance, Fig. 13a shows differences for all tested materials between model predictions and psychophysical analysis of sparkle. Major differences were recorded for samples having a fine particle size distribution (below 20 μm), especially MXB, MXW, MSB VXX1

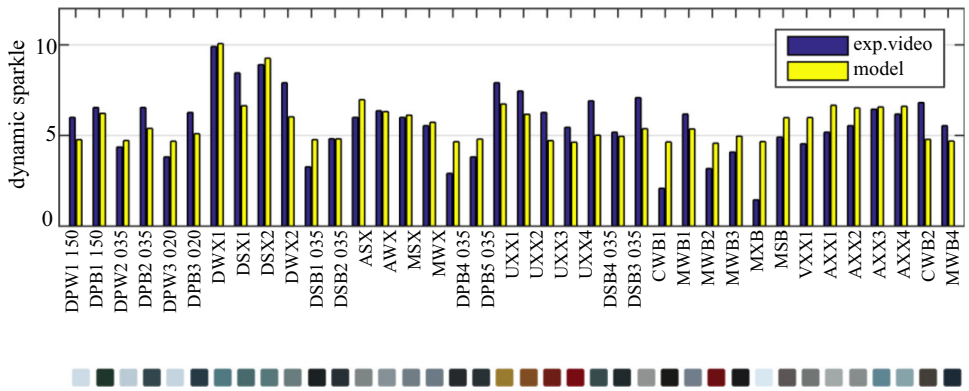

Fig. 16: A comparison of perceived dynamic sparkle obtained using a psychophysical experiment (blue bars), with its proposed model (yellow bars) (Color figure online)

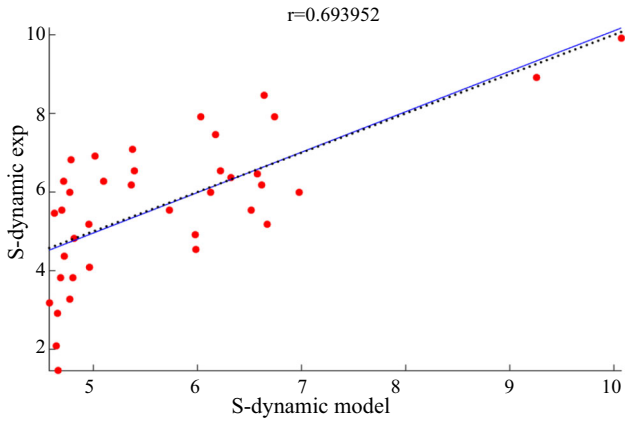

Fig. 17: A correlation plot between the dynamic sparkle model and data from the experiment with a dynamic image sequence

which are probably due to the limited spatial resolution of the imaging sensor of our goniometer. This could be the reason for the almost fixed minimal model response for those materials.

As the absolute scale of our model results differs from those of the commercial devices, we computed robust linear fit between their readings and the model outputs, resulting in offset value $c_1 = 3.99$ and scale value $c_2 = 52.72$. The final scaling of sparkle grade values using $\hat{S} = c_1 + c_2 S$ in comparison with readings of the devices is shown in Fig. 13b. The correlation value with BYK-mac was $r = 0.799$ and with MA-T12 $r = 0.650$. See Fig. 12-right for overall comparison.

Graininess model

As our goniometer cannot directly capture samples for diffuse illumination, we used a method common from computer graphics, as a linear combination of material appearance contributions for individual lights. Therefore, we approximated such illumination by computing the average image across all 151 images captured in in-plane configuration, i.e., $A = \frac{1}{N}\sum_{i=1}^{n} I_i$.

Our implementation follows the procedure suggested by Ferrero et al.[44] It combines the visual contribution of two components: (a) graininess variance and (b) sample luminance. The graininess variance is represented by a power spectral density P_A of the averaged image A. P_A was computed using Welch's method of periodogram computation in frequency domain.[45] The frequency content is then approximated by graininess variance summing up discrete frequency contributions

$$G_f = 2 \cdot \sum_{f_L}^{f_H} P_A(f), \tag{2}$$

where f_L and f_H represent the frequency range of interest.

The sample luminance factor is

$$G_l = 1 + \frac{a}{L^b}, \tag{3}$$

with a and b as fixed model parameters. The final measure of graininess is obtained by multiplication of both factors $G = G_f \cdot G_l$. For graininess assessment of our sample set, we used the parameters suggested in[44] of having a close fit to BYK-mac readings, i.e., $f_L = 1.27\,mm^{-1}$, $f_H = 1.69\,mm^{-1}$, $a = 0.12$, and $b = 0.84$. Figure 14a compares model values with psychophysical data on real samples and their photographs. The overall model's Pearson correlation with psychophysical assessment of graininess on real samples was $r = 0.790$, and with psychophysical assessment of graininess on captured images was $r = 0.750$.

Similarly to sparkle models, the absolute scales of graininess are not known. Therefore, we use readings of commercial devices on a subset of 10 samples to obtain robust linear fit between the readings and model outputs, resulting in offset value $c_3 = 3.8$ and scale value $c_4 = 1658.0$. The final scaling of graininess values

using $\hat{G} = c_3 + c_4 G$ in comparison with readings of the devices is shown in Fig. 14b. The correlation value with BYK-mac was $r = 0.651$ and with MA-T12 $r = 0.729$. See Fig. 12-left for overall comparison.

A similar approach, also based on power spectral density of image, was suggested by Kitaguchi et al.[5], where instead of summing P_A over only a limited range and using the nonlinear model of luminance factor, authors suggest P_A weighting by a contrast sensitivity function.

Implication to dynamic sparkle model

Psychophysical observations[1] have shown that, while photographs of our sample surfaces coated with different effect paints can reliably deliver information on sparkle, there is a lack of correlation between the so-called static and dynamic sparkle. Although in the previous ''Sparkle model'' section and ''Graininess model'' section, we have shown that we can obtain reasonably accurate predictions of sparkle and graininess, we are still lacking a predictor of angular sparkle dynamics. In contrast to static sparkle, a common approach to assessment of dynamic sparkle is missing. Although there might be similarities between both modalities, the dynamic sparkle is more affected by the width of the coating layer, by the orientation of particles in resin, etc.

We compared dynamic sparkle with the static sparkle observed at different illumination geometries. Figure 15 shows a graph of correlation values of perceived (a) static sparkle, i.e., between experiments on physical samples and their captured photographs (red outline), and (b) static versus dynamic sparkle, i.e., between static photographs and dynamic sparkle recorded as a video for moving light (blue outline). The average proportional change of the sample intensity is shown as a green outline. We conclude that visual assessment of static sparkle on real samples and their photographs demonstrates the highest correlation at illumination geometries close to retro-reflective angles. In contrast, visual assessment of static and dynamic sparkle from photographs has the highest correlation values for illumination geometries close to a specular highlight. This correlations drops when we approach specular reflection ($\theta_i = 30°(as\,15°)$), where individual flakes become less apparent due to the saturation of the visual system.

In a psychophysical study,[1] ten subjects were asked to assess dynamic sparkle in videos of 151 frames of 38 coating samples in a range between 0 and 10. Results of this study are shown in the blue bars of Fig. 16. We used these results as reference data for the development of our dynamic sparkle model.

In general, data from the model have less variance than those from the visual experiment. The main differences are shown for mica-based materials MWB2 and MXW.

We analyzed various measures of dynamic sparkle. A well-known measure of sparkle dynamics is the angular life-time of sparkle spots.[6] This feature, often also denoted as sparkle angular persistence, can be approximated as a count of consecutive light geometry indices where values exceed the sparkle threshold during in-plane movement of the light. This is integrated across all pixels in a coating image. This summed value across all pixels and light positions is denoted as P. Bright intensities are considered to be those exceeding stellar magnitude threshold m_t defined in ''Sparkle model'' section. The best correlation to perceived dynamic sparkle obtained from the psychophysical experiment was obtained by a combination of sparkle persistence P, average luminance L_A of the sample across all 151 illuminations geometries, and pigment particle size distribution d experimentally obtained by the optical microscope as shown in Fig. 3 $S_D = \frac{d \cdot P}{L_A}$. A Pearson correlation value of this dynamic sparkle measure to the visual data was $r = 0.634$ (p-value $1.6e{-}4$). A comparison of the model to the perceived dynamic sparkle is shown in the yellow bars of Fig. 16. However, to obtain an automatic measure, one has to replace the pigment particle size distribution d with a related computational model. To this end, we analyzed the frequency information of individual images. We applied the image variance V_I relying on power spectral density as defined in the previous ''Related work'' section; however, instead of its application to the diffuse image, we applied it directly to sparkle images, i.e., images taken with a directional illumination. To avoid bias due to the non-uniform presence of sparkle effect for all illumination angles, we computed the variance as mean values of variances obtained for different illumination geometries. We empirically derived that averaging variance close to specular reflection over a range of polar angles $\theta_i = 20 - 30°$ worked well. Using the final measure

$$S_D = \frac{V_I \cdot P}{L_A}, \tag{4}$$

we obtained correlation to perceived dynamic sparkle data $r = 0.694$ (p-value $1e{-}6$). The correlation plot is shown in Fig. 17.

An interesting aspect of visual sparkle assessment is the effect of color. As samples AXX1, AXX4 and AXX2, AXX3 have the identical pigment and differ only in color (silver and blue), we can analyze the effect of color on the perception of static and dynamic sparkle. While subjective visual responses to static

sparkle in Fig. 14 (dark blue columns) differ only slightly, we observed greater differences for dynamic sparkle in Fig. 16 (dark blue columns). As expected, the responses of the proposed models are similar in both cases regardless of the color. Although, our study was limited to a relatively low number of samples and we used dynamic stimuli of only low dynamic range, the achieved results are a promising avenue for a future analysis of dynamic sparkle.

Conclusions

This study assessed several sources of effect coating texture data. In our psychophysical studies, we compared the perceived graininess and sparkle of 38 physical samples (i.e., panels covered with effect paints including different effect pigments) and their appearance captured using a goniometer. The diffuse illumination was approximated by a sample image averaged across multiple directional illuminations. Mutual consistence of both studies has proven that image-based data convey important information on these texture effects. Furthermore, we compared the obtained psychophysical data with readings of two commercial gonioreflectometers, BYK-mac (by BYK-Gardner) and MA-T12 (by X-Rite). We obtained good correlations between human judgments and device readings for sparkle and graininess. Finally, we implemented relative measures for sparkle and graininess and compared them to the psychophysical judgments obtained in our study, and with the readings of the devices. We obtained higher correlations to perceived data of sparkle ($r = 0.87$) than for graininess ($r = 0.79$). By scaling using instrument readings, we obtained approximate standard scaling values for sparkle and graininess. Alongside the static sparkle analysis, we also analyzed its dynamic variant and proposed a relative computational model achieving promising correlation with perceived dynamic sparkle.

Acknowledgments The authors would like to thank all anonymous observers for their valuable time devoted to our psychophysical experiments.

Funding This research has been partially supported by the Czech Science Foundation Grant GA17-18407S.

Appendix

See Fig. 18 and Tables 2 and 3.

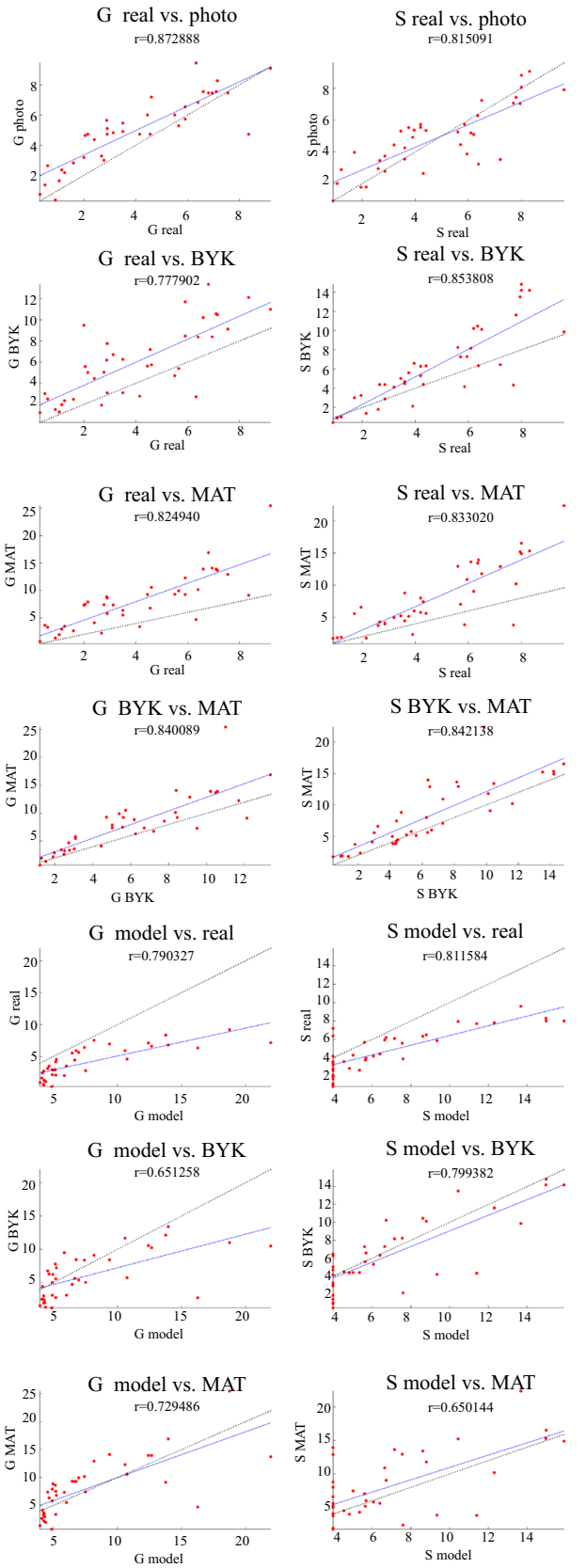

Fig. 18: Graininess and sparkle correlation charts. The blue line represents linear fit (Color figure online)

Table 2: A list of the tested effect coating samples and their composition

No	ID	Pigment type	Coating method	Basecoat color	D10 [μm]	D50 [μm]	D90 [μm]	Details
01	DPW1	Diffractive	Powder	White	45	115	210	MultiFlect 150 μm
02	DPB1	Diffractive	Powder	Black	45	115	210	MultiFlect 150 μm
03	DPW2	Diffractive	Powder	White	16	35	80	MultiFlect 35 μm
04	DPB2	Diffractive	Powder	Black	16	35	80	MultiFlect 35 μm
05	DPW3	Diffractive	Powder	White	10	21	44	MultiFlect 30 μm
06	DPB3	Diffractive	Powder	Black	10	21	44	MultiFlect 20 μm
07	DWX1	Diffractive	Water					MultiFlect medium solids
08	DSX1	Diffractive	Solvent					MultiFlect medium solids
09	DSX2	Diffractive	Solvent					MultiFlect high solids
10	DWX2	Diffractive	Water					MultiFlect high solids
11	DSB1	Diffractive	Solvent	Black	16	35	80	MultiFlect 35 μm, doctor-blade application
12	DSB2	Diffractive	Solvent	Black	16	35	80	MultiFlect 35 μm, doctor-blade application
13	ASX	Aluminum	Solvent					High solids
14	AWX	Aluminum	Water					High solids
15	MSX	Mica	Solvent					High solids
16	MWX	Mica	Water					High solids
17	DPB4	Diffractive	Powder	Black	16	35	80	MultiFlect 35 μm
18	DPB5	Diffractive	Powder	Black	16	35	80	MultiFlect 35 μm
19	UXX1	UTP			10	21	34	Zenexo GoldenShine
20	UXX2	UTP			10	21	34	Zenexo orange
21	UXX3	UTP			10	21	34	Zenexo red1
22	UXX4	UTP			10	21	34	Zenexo red2
23	DSB4	Diffractive	solvent	Black	16	35	80	MultiFlect 35 μm
24	DSB3	Diffractive	solvent	Black	16	35	80	MultiFlect 35 μm
25	CWB1	Combined	Water	Black				
26	MWB1	Mica	Water	Black				
27	MWB2	Mica	Water	Black				Xirallic T60-10
28	MWB3	Mica	Water	Black				Meoxal, Lumina Gold, Iriodin stargold, ColorStream red, Paliocrom Orange
29	MXB	Mica		Black				Xirallic T60-10
30	MXW	Mica		White				Xirallic T60-10
31	MSB	Mica	Solvent	Black				ColorShift Didpade
32	VXX1	VMP						Decomet 060412/10
33	AXX1	Aluminum			4	8	14	AluMotion S08/CAB58 8 μm
34	AXX2	Aluminum			10	22	41	AluMotion S22/CAB58 22 μm
35	AXX3	Aluminum			10	22	41	AluMotion S22/CAB57 22 μm blue
36	AXX4	Aluminum			4	8	14	AluMotion S08/CAB57 8 μm blue
37	CWB2	Combined	Water	Black				Pyrisma (red, yellow), Astrosmine, Al paste, Paliocrom Orange, ColorStream, Xirallic
38	MWB4	Mica	Water	Black				Pyrisma blue, Iriodin (satin, lilac)

Table 3: CIE Lab values of the tested coatings and results of their sparkle (S) and graininess (G) psychophysical assessment using real samples and their photographs/video

No	ID	*L*	*a*	*b*	S_{real}	S_{photo}	G_{real}	G_{photo}	S_{video}
01	DPW1	86.5	− 2.9	− 6.8	7.7	7.7	6.3	9.5	6.0
02	DPB1	20.4	− 12.6	4.2	9.6	8.3	9.2	9.1	6.5
03	DPW2	80.8	− 3.2	− 7.0	5.9	6.3	4.2	4.7	4.4
04	DPB2	28.7	− 6.7	− 6.0	8.0	7.6	7.0	7.5	6.6
05	DPW3	84.4	− 3.1	− 7.5	3.9	5.6	2.7	3.3	3.8
06	DPB3	23.4	− 4.3	− 10.0	6.4	6.8	4.5	6.0	6.3
07	DWX1	48.4	− 12.1	− 9.1	8.3	9.5	7.1	7.5	9.9
08	DSX1	42.3	− 11.1	− 5.7	8.0	8.8	6.6	7.5	8.5
09	DSX2	48.0	− 11.0	− 5.3	8.0	9.3	7.2	8.3	8.9
10	DWX2	50.8	− 6.6	− 2.9	7.8	7.8	6.4	6.8	7.9
11	DSB1	11.7	− 1.7	− 2.1	3.6	3.3	2.9	4.7	3.3
12	DSB2	19.2	− 3.5	− 3.7	5.6	5.3	4.6	7.2	4.8
13	ASX	55.0	− 3.0	− 0.8	6.2	4.2	6.8	7.5	6.0
14	AWX	59.5	− 2.9	− 4.6	5.7	3.5	5.9	6.6	6.4
15	MSX	51.7	− 3.6	− 5.4	4.0	4.5	5.9	5.7	6.0
16	MWX	50.5	− 3.1	− 7.8	3.6	3.2	4.6	4.7	5.5
17	DPB4	16.4	− 0.7	− 1.7	4.3	1.9	3.5	5.5	2.9
18	DPB5	19.5	− 3.5	− 2.9	6.0	3.0	5.5	6.0	3.8
19	UXX1	53.2	3.0	44.5	3.8	4.6	2.9	5.6	7.9
20	UXX2	37.8	17.8	33.6	3.5	3.5	3.1	4.8	7.5
21	UXX3	24.6	35.6	24.5	3.2	2.7	2.4	4.4	6.3
22	UXX4	24.5	44.3	28.6	2.9	2.8	1.6	2.8	5.5
23	DSB4	30.5	− 7.4	− 3.4	6.5	7.0	7.6	7.5	6.9
24	DSB3	15.9	− 3.4	− 2.9	6.1	4.9	5.7	5.3	5.2
25	CWB1	60.7	− 1.0	0.4	4.4	4.8	2.9	5.1	7.1
26	MWB1	8.7	− 0.6	1.6	2.0	0.9	1.2	2.4	2.1
27	MWB2	51.8	− 1.3	− 9.4	4.2	4.0	2.0	3.2	6.2
28	MWB3	22.1	39.7	24.8	2.6	1.1	0.9	0.4	3.2
29	MXB	8.9	− 0.4	− 0.4	6.4	1.1	2.8	3.0	4.1
30	MXW	90.9	− 2.6	− 6.7	2.2	0.3	0.3	0.7	1.5
31	MSB	37.0	1.7	1.4	7.2	1.8	8.4	4.7	4.9
32	VXX1	49.2	− 1.8	− 0.4	0.9	1.9	0.5	1.4	4.6
33	AXX1	68.5	− 2.5	− 1.3	1.1	2.5	1.3	2.2	5.2
34	AXX2	58.3	− 2.7	− 0.6	2.9	2.8	2.2	4.7	5.6
35	AXX3	53.2	− 10.2	− 11.2	2.7	3.3	2.1	4.6	6.5
36	AXX4	65.2	− 8.3	− 7.1	1.2	2.6	0.6	2.6	6.2
37	CWB2	26.7	0.5	5.1	4.2	4.3	3.5	4.9	6.8
38	MWB4	16.4	− 1.2	− 11.0	1.7	2.2	1.1	1.6	5.6

References

1. Filip, J, Kolafova, M, Vavra, R, ''Perceived Effects of Static and Dynamic Sparkle in Captured Effect Coatings.'' *The 15th International Conference on Signal Image Technology & Internet Based Systems, IEEE*, 2019, pp. 732–737. https://doi.org/10.1109/SITIS.2019.00119.
2. Pfaff, G, Reynders, P, ''Angle-Dependent Optical Effects Deriving from Submicron Structures of Films and Pigments.'' *Chem. Rev.*, **99** (7) 1963–1982 (1999)
3. Maile, F, J, Pfaff, G, Reynders, P, ''Effect Pigment—Past, Present and Future.'' *Prog. Org. Coat.*, **54** (3) 150–163 (2005)
4. Pfaff, G, *Special Effect Pigments: Technical Basics and Applications*. Vincentz Network GmbH & Co KG, Hannover (2008)
5. Kitaguchi, S, Luo, MR, Kirchner, EJ, van den Kieboom, G-J, ''Computational Model for Perceptual Coarseness Prediction.'' *Conference on Colour in Graphics, Imaging, and Vision*, Vol. 2006, Society for Imaging Science and Technology, pp. 278–282 (2006)
6. Kirchner, E, van den Kieboom, G.-J, Njo, L., Supèr, R, Gottenbos, R, ''Observation of Visual Texture of Metallic and Pearlescent Materials.'' *Color Res. Appl.*, **32** (4) 256–266 (2007)
7. Huang, Z, Xu, H, Luo, M, R, Cui, G, Feng, H, ''Assessing Total Differences for Effective Samples Having Variations in Color, Coarseness, and Glint.'' *Chin. Opt. Lett.*, **8** (7) 717–720 (2010)
8. Rentschler, T, ''Measuring Sparkling Blues Without Blues.'' *Eur. Coat. J.*, **12** 78–83 (2011)

9. Dekker, N, Kirchner, E, Super, R, van den Kieboom, G, Gottenbos, R, ''Total Appearance Differences for Metallic and Pearlescent Materials: Contributions from Color and Texture.'' *Color Res. Appl.*, **36** (1) 4–14 (2011)
10. Kirchner, E, Ravi, J, ''Setting Tolerances on Color and Texture for Automotive Coatings.'' *Color Res. Appl.*, **39** (1) 88–99 (2014)
11. Kirchner, E, Van der Lans, I, Perales, E, Martínez-Verdú, F, Campos, J, Ferrero, A, ''Visibility of Sparkle in Metallic Paints.'' *JOSA A*, **32** (5) 921–927 (2015)
12. Wang, ZW, Luo, MR, ''Looking into Special Surface Effects: Diffuse Coarseness and Glint Impression.'' *Color. Technol.*, **132** (2) 153–161 (2016)
13. Seubert, C, Nichols, M. Frey, J, Shtein, M, Thouless, M, ''The Characterization and Effects of Microstructure on the Appearance of Platelet-Polymer Composite Coatings.'' *J. Mater. Sci.*, **51** (5) 2259–2273 (2016)
14. Seubert, C, Nichols, M, Kappauf, C, Ellwood, K, Shtein, M, Thouless, M, ''A Hybrid Ray-wave Optics Model to Study the Scattering Behavior of Silver Metallic Paint Systems.'' *J. Coat. Technol. Res.*, **15** (3) 471–480 (2018)
15. Gómez, O, Perales, E, Chorro, E, Viqueira, V, Martínez-Verdú, FM, ''Visual and Instrumental Correlation of Sparkle by the Magnitude Estimation Method.'' *Appl. Opt.*, **55** (23) 6458–6463 (2016)
16. Iacomussi, P, Radis, M, Rossi, G, ''Brightness and Sparkle Appearance of Goniochromatic Samples.'' *Proceedings of the IS&T International Symposium on Electronic Imaging, MMRMA*, pp. 365.1–365.6 (2016)
17. Amookht, S, Kandi, SG, Mahdavian, M, ''Quantification of Perceptual Coarseness of Metallic Coatings Containing Aluminum Flakes Using Texture Analysis and Visual Assessment Methods.'' *Prog. Org. Coat.*, **137** 105375 (2019)
18. Watanabe, S, ''One-Shot Multi-angle Measurement Device for Evaluating the Sparkle Impression.'' *Electron. Imaging*, **2020** (5) 60401–1 (2020)
19. Perales, E, Micó-Vicent, B, Huraibat, K, Viqueira, V, ''Evaluating the Graininess Attribute by Visual Scaling for Coatings with Special-Effect Pigments.'' *Coatings*, **10** (4) 316 (2020)
20. Ferrero, A, Basic, N, Campos, J, Pastuschek, M, Perales, E, Porrovecchio, G, Šmid, M, Schirmacher, A, Velázquez, J, Martínez-Verdú, F, ''An Insight into the Present Capabilities of National Metrology Institutes for Measuring Sparkle.'' *Metrologia*, **57** (6) 065029 (2020)
21. Günther, J, Chen, T, Goesele, M, Wald, I, Seidel, H-P, ''Efficient Acquisition and Realistic Rendering of Car Paint.'' *VMV* pp. 487–494 (2005)
22. Ershov, S, Kolchin, K, Myszkowski, K, ''Rendering Pearlescent Appearance Based on Paint-Composition Modelling.'' *Comput. Graph. Forum*, **20** (3) 227–238 (2001)
23. Ďurikovič, R, Martens, WL, ''Simulation of Sparkling and Depth Effect in Paints.'' *Proceedings of the 19th Spring Conference on Computer Graphics, SCCG '03*, ACM, New York, NY, USA, pp. 193–198 (2003)
24. Ergun, S, Önel, S, Ozturk, A, ''A General Micro-Flake Model for Predicting the Appearance of Car Paint.'' *Proceedings of the Eurographics Symposium on Rendering: Experimental Ideas & Implementations, EGSR '16*, pp. 65–71 (2016)
25. Ďurikovič, R, Mihálik, A, ''Metallic Paint Appearance Measurement and Rendering.'' *J. Appl. Math. Stat. Inf.*, **9** (2) 25–39 (2007)
26. Rump, M, Muller G, Sarlette, R, Koch, D, Klein,R, ''Photo-Realistic Rendering of Metallic Car Paint from Image-Based Measurements.'' *Comput. Graph. Forum*, **27** (2) 527–536 (2008)
27. Rump, M, Sarlette, R, Klein, R, ''Efficient Resampling, Compression and Rendering of Metallic and Pearlescent Paint.'' In: Magnor, M, Rosenhahn, B, Theisel H (eds.), *Vision, Modeling, and Visualization*, pp. 11–18 (2009)
28. Golla, T, Klein, R, ''An Efficient Statistical Data Representation for Real-Time Rendering of Metallic Effect Car Paints.'' In: Barbic, J. D'Cruz, M, Latoschik, ME, Slater, M, Bourdot P, (eds.) *Virtual Reality and Augmented Reality*, Springer International Publishing, pp. 51–68 (2017)
29. Lans, Ivd, Kirchner, E, Half, A, ''Accurate Appearance-Based Visualization of Car Paints.'' *Proceedings of International Conference on Computer Graphics*, pp. 17–23 (2012)
30. Kirchner, E, Ravi, J, ''Predicting and Measuring the Perceived Texture of Car Paints.'' In: Padilla, S, Chantler, MJ, Harris, JM, & Pointer, MR Lulu (eds.) *Predicting Perceptions: Proceedings of the 3rd International Conference on Appearance*, pp. 25–28 (2012)
31. Ferrero, A, Campos, J, Rabal, A, Pons, A, ''A Single Analytical Model for Sparkle and Graininess Patterns in Texture of Effect Coatings.'' *Opt. Express*, **21** (22) 26812–26819 (2013)
32. Kirchner, E, van der Lans, I, Koeckhoven, P, Huraibat, K, Martínez-Verdú, F, Perales, E, Ferrero, A, Campos, J, ''Real-time Accurate Rendering of Color and Texture of Car Coatings.'' *Electron. Imaging Color Imaging XXIV: Display. Process. Hardcopy Appl.*, pp. 76–1–76–6(6) (2019). https://doi.org/10.2352/ISSN.2470-1173.2019.14.COLOR-076.
33. McCanny, CS, ''Observation and Measurement of the Appearance of Metallic Materials. Part. 1. Macro Appearance.'' *Color Res. Appl.*, **21** (4) 292–304 (1996)
34. E2194-12, A, *Standard Practice for Multiangle Color Measurement of Metal Flake Pigmented Materials*. West Conshohocken PA, ASTM International (2012)
35. E2539-12, A, *Standard Practice for Multiangle Color Measurement of Interference Pigments*. West Conshohocken PA, ASTM International (2012)
36. BYK-mac i COLOR product information, BYK-Gardner GmbH, https://www.byk-instruments.com/cz/en/color/byk-mac-i-metalliccolor/c/2338, accessed 14/6/2020
37. MA-T12 multiangle spectrophotometer product information, X-Rite, https://www.xrite.com/categories/portable-spectrophotometers/ma-t12, accessed 14/6/2020
38. Keelan, B, ''ISO 20462: A Psychophysical Image Quality Measurement Standard.'' *Proceedings of the SPIE*, vol. 5294, SPIE 2003, pp. 181–189 (2003)
39. Filip, J, Vávra, R, Haindl, M, Zid, P, Krupicka, M, Havran, V, ''BRDF Slices: Accurate Adaptive Anisotropic Appearance Acquisition.'' *Proceedings of the 26th IEEE Conference on Computer Vision and Pattern Recognition, CVPR 2013* pp. 4321–4326 (2013)
40. Hayes, AF, Krippendorff, K, ''Answering the Call for a Standard Reliability Measure for Coding Data.'' *Commun. Methods Meas.*, **1** (1) 77–89 (2007)
41. ITU, *ITU-R.REC.P.910. Subjective Audivisual Quality Assessment Methods for Multimedia Applications*, Tech. Rep., International Telecommunication Union (2008)
42. Kitaguchi, S, Luo, MR, Westland, S, Kirchner, EJ, van den Kieboom, G-J, ''Assessing Texture Difference for Metallic Coating on Different Media.'' *Color and Imaging Conference*, Vol. 2006, Society for Imaging Science and Technology, pp. 197–202 (2006)
43. Crumey, A, ''Human Contrast Threshold and Astronomical Visibility.'' *Mon. Not. R. Astron. Soc.*, **442** (3) 2600–2619 (2014)

44. Ferrero, A, Velázquez, JL, Perales, E, Campos, J, Verdú, FMM, ''Definition of a Measurement Scale of Graininess from Reflectance and Visual Measurements.'' *Opt. Express*, **26** (23) 30116–30127 (2018). https://doi.org/10.1364/OE.26.030116.
45. Welch, P, ''The Use of Fast Fourier Transform for the Estimation of Power Spectra: A Method Based on Time Averaging Over Short, Modified Periodograms.'' *IEEE Trans. Audio Electroacust.*, **15** (2) 70–73 (1967). https://doi.org/10.1109/TAU.1967.1161901.